SERS-based Quantification of PSMA in Tissue Microarrays Allows Effective Stratification of Patients with Prostate Cancer

Manjari Bhamidipati[†], Geuntaek Lee[ζ], Isaac Kim[ζ], and Laura Fabris*[, §]

[†]Department of Biomedical Engineering, Rutgers University, 599 Taylor Road, Piscataway NJ 08854

[ζ]Cancer Institute of New Jersey-Urology Oncology, Rutgers University, 120 Albany Street, New Brunswick, NJ 08901

[§]Department of Materials Science and Engineering, Rutgers University, 607 Taylor Road, Piscataway, NJ 08854

Supporting Information

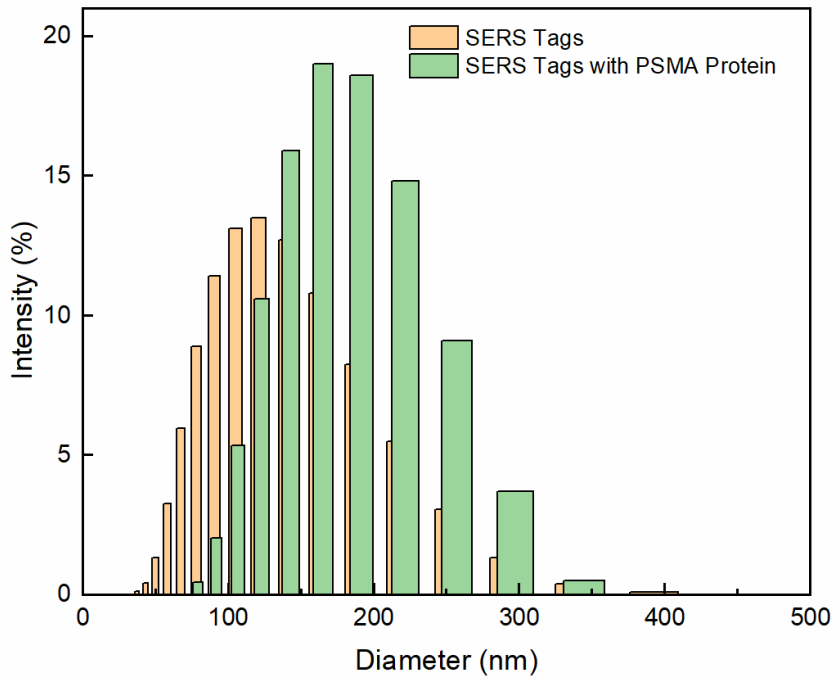

Figure S1: Dynamic light scattering (DLS) data reporting size distribution analysis of SERS tags (gold nanostars functionalized with 4-ATP and PSMA aptamer) and SERS tags after recognition and binding of soluble PSMA. The results indicate an increase in size, implying that the PSMA aptamer function is still intact even after bioconjugation to the gold nanostars.

Particles	Amount of RNA on NP (µg)	RNA Added (µg)	Capture Efficiency (%)
1.5 nM NS_0.5 µM 4ATP_ 0.5 µM Apt	2.27 ± 0.06	2.34 ± 0.02	48.48 ± 1.29
1.5 nM NS_1 µM 4ATP_0.5 µM Apt	1.77 ± 0.08	2.34 ± 0.02	37.79 ± 1.88
1.5 nM NS_2 µM 4ATP_ 0.5 µM Apt	1.68 ± 0.09	2.34 ± 0.02	35.94 ± 2.06
3 nM NS_0.5 µM 4ATP_0.5 µM Apt	1.99 ± 0.03	4.68 ± 0.04	42.56 ± 0.74
3 nM NS_1 µM 4ATP_0.5 µM Apt	2.34 ± 0.02	4.68 ± 0.04	50.02 ± 0.53
3 nM NS_2µM 4ATP_0.5 µM Apt	2.46 ± 0.01	4.68 ± 0.04	52.56 ± 0.23

Figure S2: Capture efficiency of PSMA RNA aptamer on the nanoparticles calculated using the Quant-iT™ OliGreen® ssDNA kit. Two different concentrations of gold nanostars (1.5 nM and 3 nM) were functionalized with varying ratios of the Raman reporter, 4ATP, and PSMA aptamer. Results are shown as mean ± standard deviation with n = 3 readings for each sample.

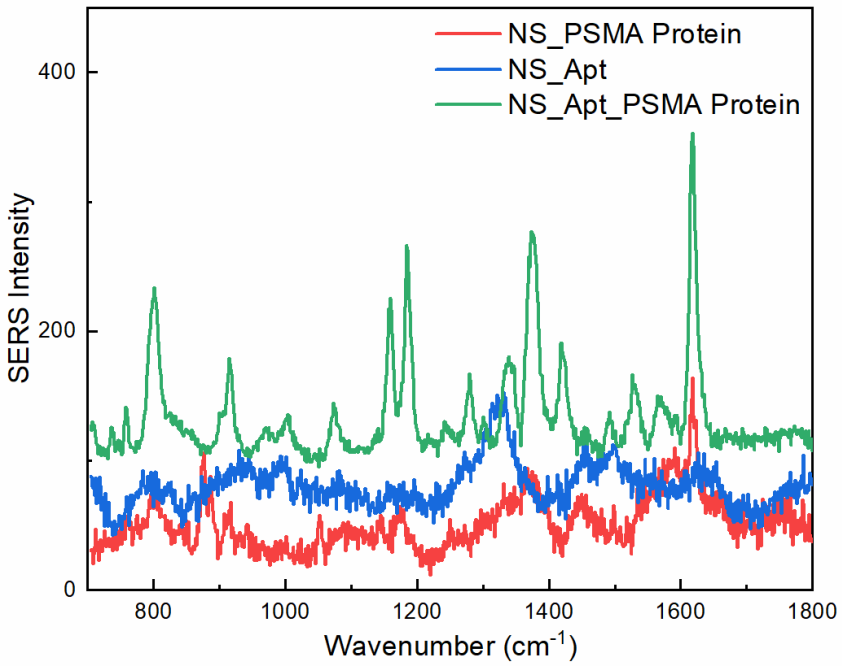

Figure S3: After recognition and binding of PSMA to the aptamer, a clear SERS spectrum emerges. The peak pattern can be uniquely assigned to the aptamer and the protein.

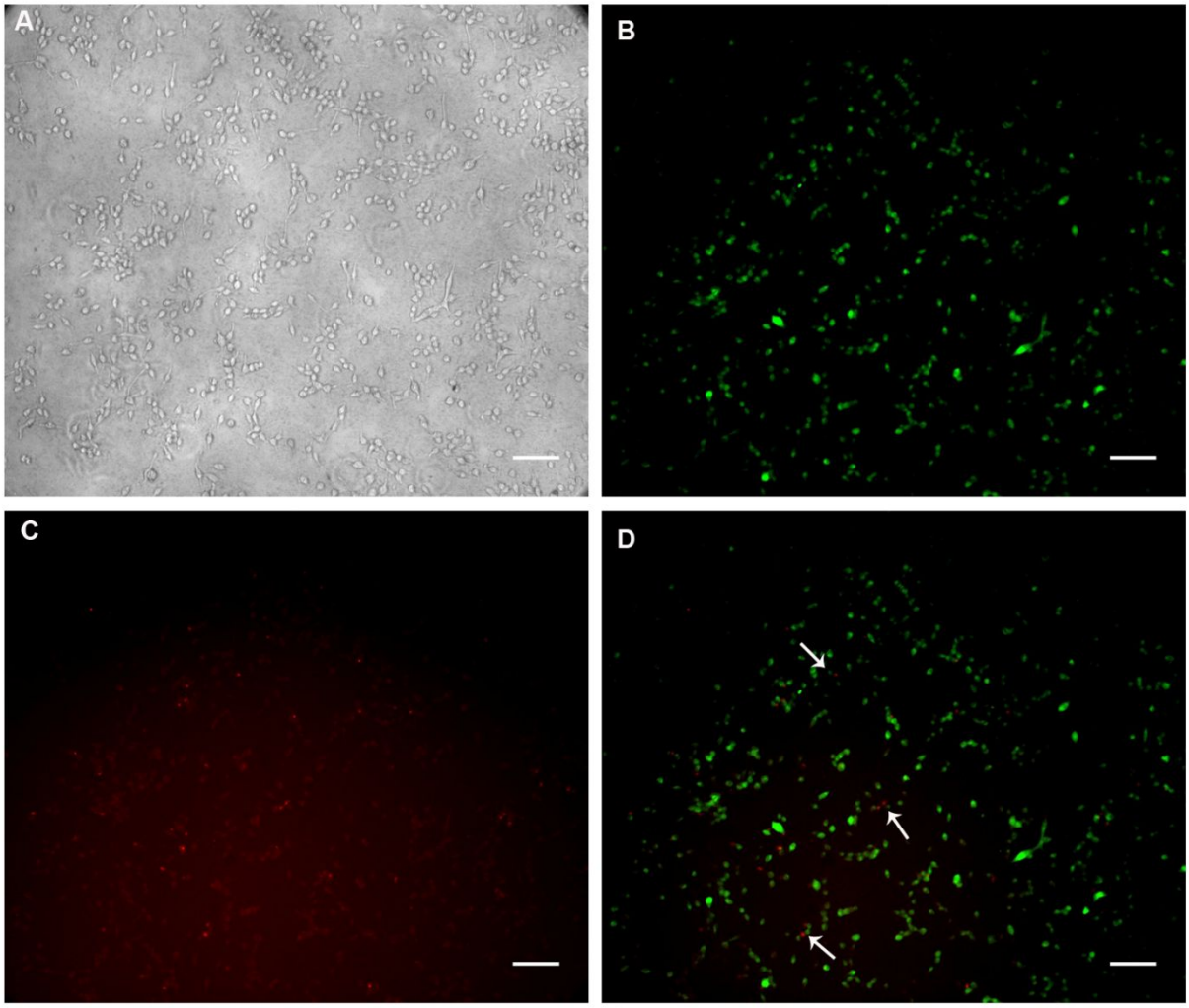

Figure S4: A) Bright field image of LNCaP cells. B) The cells were stained with a PSMA antibody that was conjugated to the fluorophore, Alexa Fluor 488. The cells were then incubated with a 3 nM concentration of SERS tags that was conjugated with a Cy3 dye, seen in panel C). Panel D) shows a composite image of the PSMA expression seen in the LNCaP cells and the SERS tags. The arrows indicate where the nanoparticles interact with the PSMA expressed on the cells. Scale bars represent 200 μm.

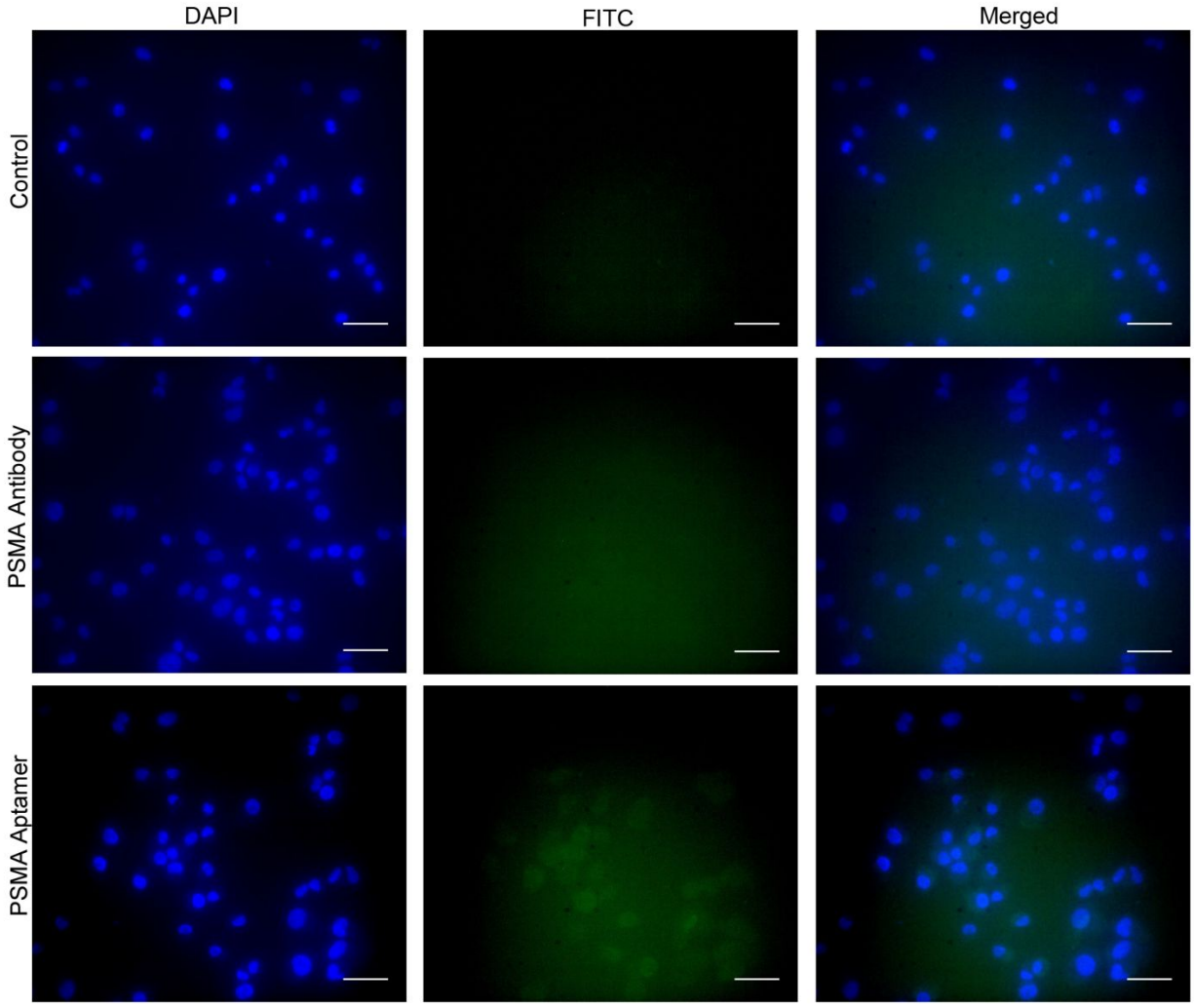

Figure S5: Fluorescent staining of PC3 cells with PSMA antibody and PSMA aptamer, both conjugated to the fluorophore, Alexa Fluor 488. Cell nuclei were stained with DAPI. Control represents cells that weren't stained with PSMA aptamer or antibody. Scale bars 50 μm.

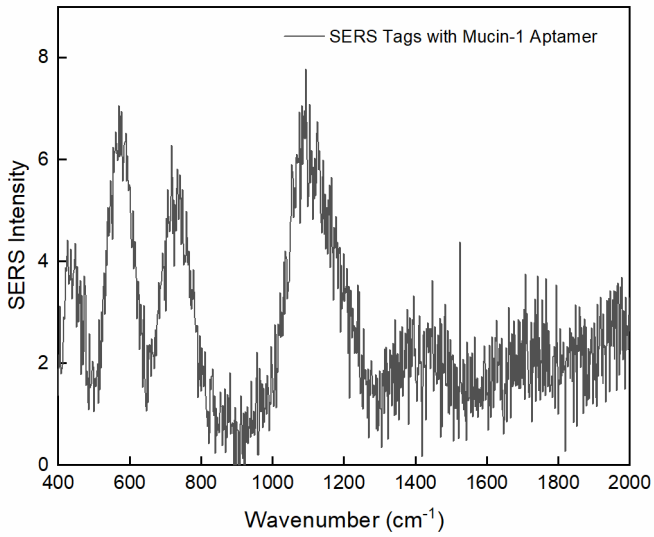

Figure S6: SERS spectrum of LNCaP cells treated with SERS tags functionalized with a nonspecific aptamer, Mucin-1. Clearly no substantial signal originates in this case, signifying that no SERS tags (or only a few, non-specifically) bind to the cell in the absence of the appropriate aptamer.

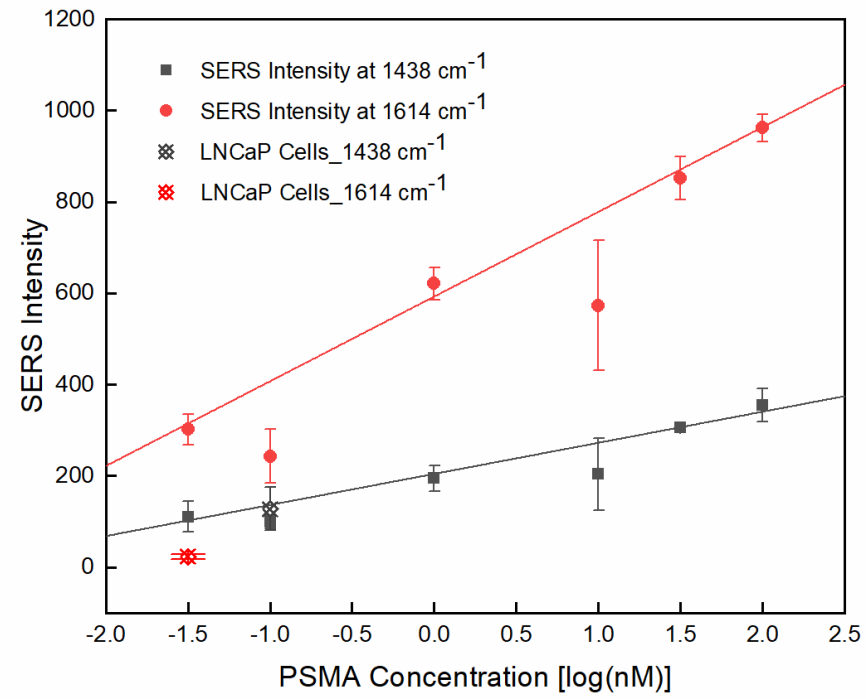

Figure S7: SERS peak intensities at 1438 cm^{-1} and 1614 cm^{-1} observed for different PSMA protein concentrations. The concentration curve generated with the 1438 cm^{-1} peak was used to estimate the PSMA expression on individual LNCaP cells. The intensity values for the LNCaP cells observed at 1614 cm^{-1} were out of the concentration range used to generate the curve.

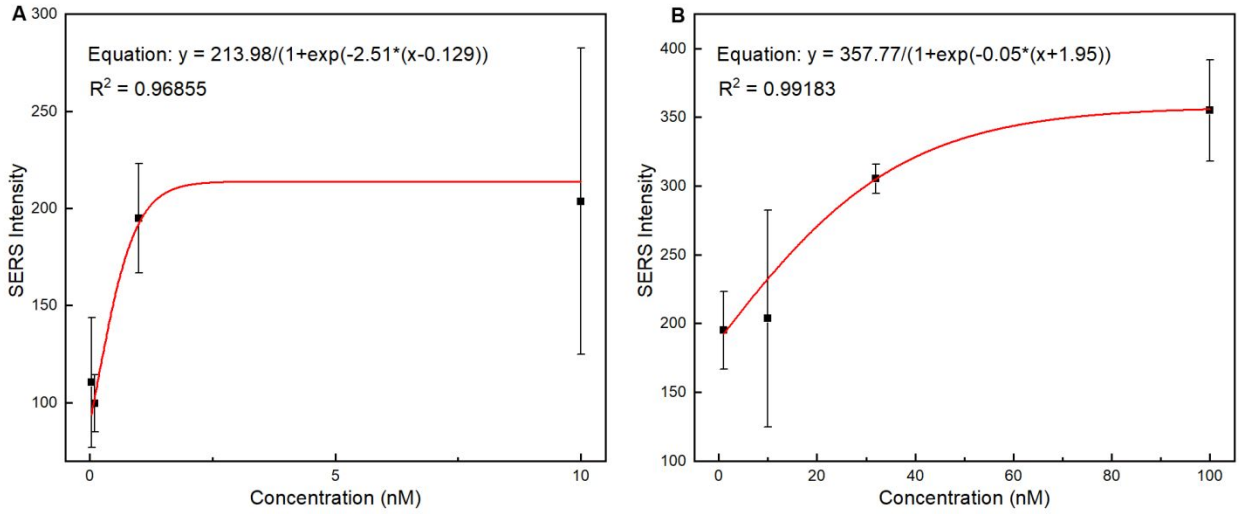

Figure S8: Binding affinity curves for the PSMA aptamer within the 32 pM-100 nM soluble PSMA concentration range. The best fit between them was obtained using a 1-parameter logistic binding model curve that is defined by the equation y = a/(1+exp((-k*(x-x_c))). Based on the fit, two dissociation constants (1/k) were determined. The first one was in the low concentration range of 32 pM to 10 nM with k_{D1} = 0.39 nM while the second dissociation constant was found to be in the higher concentration range of 1 nM and 100 nM with k_{D2} = 20 nM.

Calculation of Error on Enhancement Factor based on Nanostar Polydispersity

The surface area of gold nanostars was calculated using the equation below [1]:

$$A = 4\pi a^2 - \sum_{i=1}^{n}\left\{2\pi a\left(a - \sqrt{a^2 - R_i^2}\right\}\right. + \sum_{i=1}^{n}\left\{\pi(r_i + R_i)\sqrt{(R_i - r_i)^2 + h_i^2} + 2\pi r_i^2\right\}$$

where a = radius of the spherical core

R = base radius of a spike

r = radius of the hemispherical tip of a spike

h = distance between R and r

Using this equation, the average surface area of the synthesized gold nanostars was calculated to be A_{AV}= 18770 ± 7406 nm^2 with a standard deviation of 39%.

Therefore, considering that:

$EF = (I_{SERS}/I_{Raman}) \times (N_{Raman}/N_{SERS})$

and that [2]:

N_{SERS}= (molar surface coverage x $N_{Avogadro}$ x laser spot size)

The variation in EF will be proportional to $1/N_{SERS}$ and therefore to $1/A_{nanostars}$. If we calculate the standard deviation in EF based on the standard deviation in surface area alone (not taking into account additional variability and therefore simplifying error propagation), we derive a SD in EF that follows the relationship:

$$\delta EF = |EF| [(\delta A/A)^2]^{1/2} = EF [(97406/18770)^2]^{1/2} = 0.15\ EF$$

Which corresponds to a 15% SD in the measurements. Based on this number, the variability observed in the SERS signal of the tissues cannot be attributed to variability in EF caused by the polydispersity of the nanostars, but to actual tissue heterogeneity and variability in the expression of PSMA.

References

[1] Tsoulos, T. V.; Han, L.; Weir, J.; Xin, H. L.; Fabris, L. A Closer Look at the Physical and Optical Properties of Gold Nanostars: An Experimental and Computational Study. *Nanoscale* **2017**, *9*, 3766.

[2] Indrasekara, A. S. D.S.; Meyers, S.; Shubeita, S.; Feldman, L. C.; Gustafsson, T.; Fabris, L. Gold Nanostar Substrates for SERS Sensing in the Femtomolar Regime. *Nanoscale* **2014**, *6*, 8891.